DESIGN OF PERMANENT MAGNET LINEAR BRUSHLESS D.C. MOTOR WITH PRINTED CIRCUIT ARMATURE

Özgür ÜSTÜN **R.Nejat TUNÇAY**
İstanbul Teknik Üniversitesi, Elektrik-Elektronik Fakültesi
Elektrik Mühendisliği Bölümü, 80626 Maslak, İSTANBUL TÜRKİYE
ustun@elk.itu.edu.tr, tuncay @ elk.itu.edu.tr

ABSTRACT

This study involves the design of linear brushless d.c. motor with printed circuit armature. Initially various design topologies and properties of various permanent magnets are studied. The double-sided linear motor is chosen such that, two NdFeB magnet assembly with steel back irons and a printed circuit armature between magnets are used.

The finite element method is employed for electromagnetic field analysis and, magnetic quantities are calculated. The effect of design parameters are evaluated. The lumped parameter dynamic modeling of the motor and its control network is achieved in VisSim™ environment and the performance characteristics are calculated. The test motor is constructed and tested. The developed new design concepts are evaluated experimentally. It is believed that, this topology will offer advantages over conventional types for intelligent linear motion applications.

1. STRUCTURE OF THE MOTOR

The developed motor is a double-sided linear brushless d.c. motor (DSLBDCM) in which, two rare-earth permanent magnets with solid steel back iron constitute the excitation and, printed-circuit planar coils constitute the armature. As a result of the various initial design and topology studies, it is decided that NdFeB magnet is suitable for such high air gap topologies [1,2]. The simplified cross-section of the motor is shown in Figure.1. As it is seen, four pole type is used which is believed to be adequate to assume uniform flux distribution in the air gap. For higher number of poles, this assumption is easily justified.

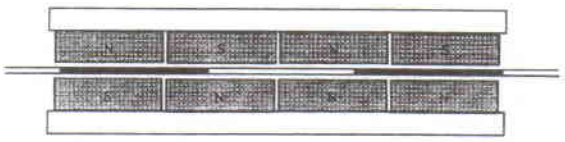

Fig.1. The cross-section view of DSLBDCM.

The NdFeB permanent magnets (PM) are mounted on solid steel back irons. These irons should be strong enough to resist the attraction force between two oppositely polarized magnets at the each part of exciters. For this design, PM assemblies are the stationary and the armature is the moving member. The armature winding is a double faced printed circuit in which, each face are insulated from each other, but connected from the ends of the windings. The leads of each coil is taken out such that, it is possible to supply the coils individually. Therefore electronic power supply can control the coil currents to produce high quality brushless d.c. performance. The armature winding is very light, thus mechanical time constant is very low which is desirable for most of the motion control systems. Ignoring the role of the back iron, this is the coreless topology, which eliminates the reluctance and cogging forces as well as increases the force to weight ratio. The picture of one armature printed circuit board is shown in Figure 2.

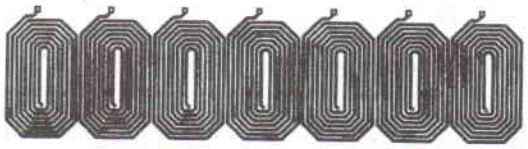

Fig. 2. Printed circuit armature windings.

Substantial effort has gone into the investigation of the effect of the sizes of the gap length, magnets and other similar quantities. This study is presented in chapter three. Although it is relevant, it should be mentioned in this part of the paper that, this topology enables to increase the output force by increasing the number of planar printed circuit boards. It is believed that this is a useful tool to provide flexible designs without changing the major quantities of the motor. Otherwise, this would have been very costly.

Another initial decision during the design that, whether moving member is armature or magnet assembly. The moving armature type is chosen since this topology provides quick response facility.

2. MAGNETIC FIELD ANALYSIS

The magnetic field analysis of the motor is achieved by employing Finite Element Method (FEM) package in Cartesian coordinates. As it is known that FEM is a numerical method which solves the Maxwell equations numerically.

For the field analysis, the properties of the magnets are stored in FEM program and automatic mesh generation procedure is used and the vector potentials and magnetic flux densities in various parts of the magnetic circuit are computed.[3]

The magnetic field of the motor has two sources: the vector density of current in planar windings

$$\vec{J} = J.\vec{k} \tag{1}$$

and the magnetization vector of NdFeB magnets

$$M_0 = M_{0x}\,\vec{i} + M_{0y}\,\vec{j} \tag{2}$$

which is not time-dependent. It is assumed that the magnetic field is two dimensional, and characterized by a vector potential $\vec{A}$, flux density $\vec{B}$, and field intensity $\vec{H}$. It is known that;

$$\vec{H} = \frac{1}{\mu}\vec{B} - \frac{1}{\mu}\vec{M}_0 \tag{3}$$

where μ is the magnetic permeability of medium.

Magnetic characteristics of the back iron and permanent magnets are single valued. The vector potential $\vec{A}$ satisfies Poisson's non-linear differential equation,

$$\frac{\partial}{\partial x}\left(\frac{1}{\mu}\frac{\partial A}{\partial x}\right) + \frac{\partial}{\partial y}\left(\frac{1}{\mu}\frac{\partial A}{\partial y}\right) = -(J + J_m) \tag{4}$$

where

$$J_m = rot_z\left(\mu^{-1}\vec{M}_0\right) = \frac{\partial(\mu^{-1}M_{0y})}{\partial x} - \frac{\partial(\mu^{-1}M_{0x})}{\partial y} \tag{5}$$

Equation(4) solved by using FEM. The flux lines of motor shown in Figure.3. The magnetic thrust force acting on windings is calculated by using Lorentz force equation.

$$\vec{F} = \int_V \vec{B} \times \vec{J}.dV \tag{6}$$

Figure 3. The magnetic flux lines of motor.

3. OPTIMAL DESIGN CONCEPT

The force produced by the motor is the product of armature ampere turns and magnetic flux density in air gap. Since the air gap flux is produced by permanent magnets, the actual flux value depends upon the demagnetization characteristic of the magnet and the load line. Obviously, one way to increase the force is to increase the armature ampere-turns which is possible by increasing the current and/or number of turns. The allowed current density in flat surface coils in printed circuit is very high, thus a high armature current can flow in this configuration. However, because of the high joule losses and excessive heating, it is not advisable to increase the current density further for continuous operation. The excessive heat also deteriorate the B-H curve of magnet and causes lower gap flux density and lower force. NdFeB magnets are particularly sensitive to temperature rise. A very high energy coefficient of NdFeB magnets at room temperature becomes very low at temperatures above 80^0C. Since joule loss of armature coil is proportional with the square of armature current, increasing the current to improve the force is not appropriate solution for especially temperature dependent permanent magnets such as NdFeB magnets. Therefore, for a good design, only way to increase the armature ampere-turns is to increase the number of turns.

Since the armature winding is a flat printed circuit, number of turns is increased by adding parallel printed circuit boards. In order to insert a number of boards into the gap, gap length in normal direction should be increased. This yields reduction in the slope of the load line and reduction in magnetic flux density produced by the magnet. The ideal operating point for PM's is the point which produce maximum product of magnetic flux density and magnetic field intensity -$(B.H)_{max}$-. For the NdFeB magnets the coordinates of this point is $(H_c/2;B_r/2)$ at the room temperature. However, for this type of motor the operation point is far beyond that point. In Figure 4, operating points are shown between demagnetization curve of the magnet and the operating lines representing variable gap lengths for increased ampere-turns at constant armature current.

The output force is calculated for various number of turns and their corresponding air gap magnetic flux densities. Force versus corresponding gap flux density curve is shown in Figure 5.

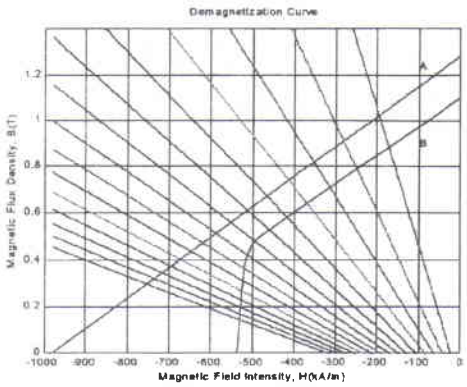

Figure 4. The variation of the operating point with increasing number of turns at constant current, demagnetization curve at the room temperature (A), demagnetization curve at 100^0C (B).

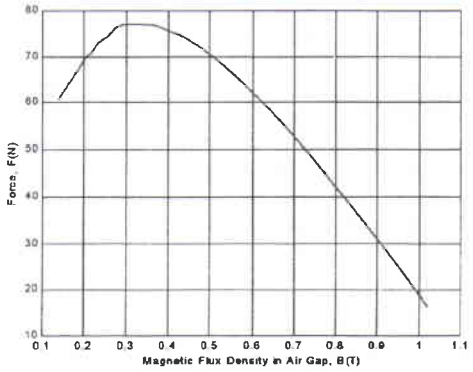

Figure 5. Force versus air gap flux density.

It is seen that there is an optimum magnetic flux density to produce maximum force, and this point is smaller than $B_r/2$. Because of the structure of the motor, the optimum operating point is quietly far from the ideal case. In addition the effect of temperature rise should be taking into account therefore an accurate prediction of the joule losses of the armature winding becomes crucial.[4]

4. MODELLING OF DSLBDCM BY TAKING DEMAGNETIZATION INTO ACCOUNT

At the room temperatures, the demagnetization characteristic of NdFeB magnet is a straight line and modeled as:

$$B_m = B_r\left(1 - \frac{H_m}{H_c}\right) \tag{7}$$

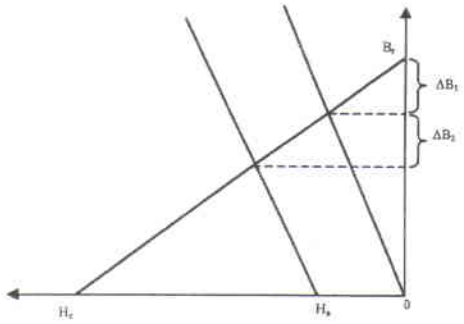

Figure 6. Characterization of structural and load demagnetization.

The load line position depends on magnet and air gap sizes:

$$B_m = -2\mu_0 \frac{l_m}{l_g} H_m \tag{8}$$

The demagnetization characteristic of the permanent magnet has two distinct effects. ΔB_1 and ΔB_2 are representing magnetic circuit mmf and load mmf effects, respectively.

ΔB_1 depends on structural parameters such as magnet depth and air gap length and it is constant for coreless motors. It is obtained as:

$$\Delta B_1 = B_r - \frac{B_r}{1 + \dfrac{B_r}{2\mu_0 \dfrac{l_m}{l_g} H_c}} \tag{9}$$

ΔB_2 depends on armature magnetic field intensity, e.g. armature current, number of turns and magnet depth. It is obtained as:

$$\Delta B_2 = \frac{B_r H_a}{H_c + \dfrac{B_r}{2\mu_0 \dfrac{l_m}{l_g}}} \tag{10}$$

The air gap magnetic flux density is determined by those demagnetization values.

$$B_g = B_r - \left(\Delta B_1 + \Delta B_2\right) \tag{11}$$

Therefore the force equation,

$$F = k_1 I_a - k_2 I_a^2 \tag{12}$$

and electromotive force,

$$E_a = k_1 v - k_2 v I_a \qquad (13)$$

where k_1 and k_2 motor coefficients are obtained.

In Equation (12) k_2 is proportional to square of number of turns of armature windings. The $k_2 I_a^2$ term corresponds to the reduction in force caused by the effect of loading demagnetization. Equation (12) clearly shows that increasing armature ampere-turns does not always yield same improvement in output force. Especially, demagnetization should be taken in to account when modeling the motors having high ampere-turns.

In order to calculate the performance characteristics of motor, VisSim™ model is formed. This model takes the electrical and mechanical quantities into account. In Figure.7. the VisSim™ model of DSLBDCM is presented.

The simulation study yields number of results. Among those, force-current variation is most important one. In order to evaluate the correlation between the theoretical and experimental results, force versus current curve will be presented together with that of experiment in the next chapter.

5. EXPERIMENTAL RESULTS

An experimental setup is formed, armature coils are supplied by power supply via power electronic circuit. The thrust force, input current and voltage are recorded. The force-current graphic is given in Figure.8. which shows a very good linear relationship between force and current. This is very encouraging since control is very straightforward. The test motor has one layer of printed circuit armature. So the demagnetization effect caused by the armature magnetic field intensity is relatively low.

Since there is no continuous motion in such type of machines and even motor speed is almost zero in most of the applications., the output power is not defined. Efficiency definition in conventional way is no longer valid. Instead, the force to input power (F/P_1) ratio is proposed hitherto as a quality measure [5,6,7]. The F/P_1 versus current curve of the motor is presented in Figure.9.

6. CONCLUSION

The design parameters of the permanent magnet double-sided linear brushless d.c. motor with printed circuit armature have been established. Finite element field calculations and the simulation of the motor in VisSim™ environment have been presented. Designed motor has manufactured and tested. The correlation between simulation and experimental results have found to be satifactory. The effect of design parameters on performance of motor has been evaluated.

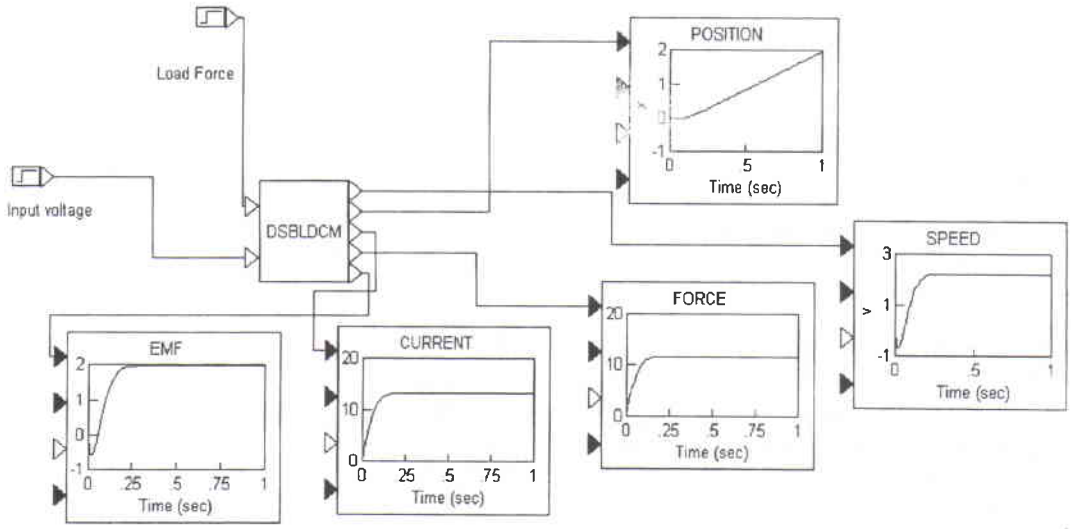

Figure.7. The model of DSLBDCM and various electrical and mechanical parameters of the motor.

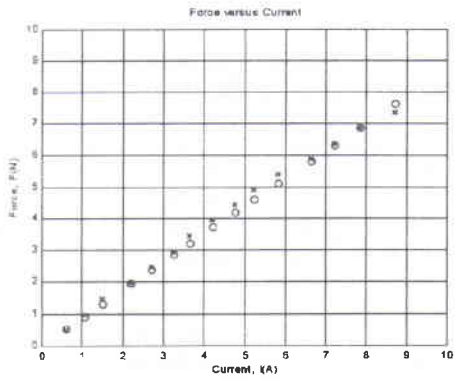

Figure 8. Force versus armature current graphic.
(x) Experimental values.
(o) Simulation values.

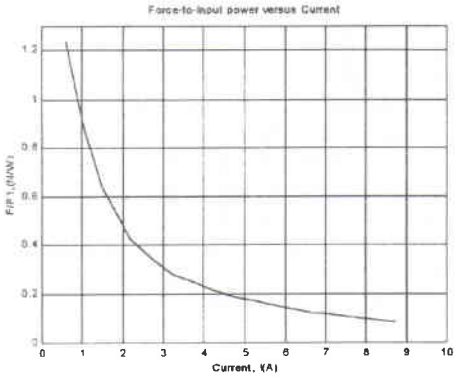

Figure 9. Force to input power ratio (F/P_1) versus armature current.

LIST OF SYMBOLS

J : Current density
M_0 : Magnetization
A : Vector potential
F : Force
μ : Permeability of magnetic medium
μ_0 : Permeability of vacuum
V : Volume
H_c : Coercivity
B_r : Remenance
l_m : Depth of magnet
l_g : Length of air gap
B_m : Magnetic flux density at the operating point
H_m : Magnetic field intensity at the operating point
I_a : Armature current
E_a : Armature emf
k_1 : Motor coefficient
k_2 : Motor coefficient
ΔB_1: Structural demagnetization
ΔB_2: Loading demagnetization

ACKNOWLEDGEMENTS

Authors are grateful to The Science and Technological Research Council of Turkey (TÜBİTAK) for providing financial support under EEEAG 197E047 project.

REFERENCES

[1] Basak, A., Permanent-Magnet D.C. Linear Motors, Oxford, Clarendon Press, 1996.
[2] Hippner, M., Piech, Z., Ripple Free Linear Synchronous Motor, ICEM'98, pp. 845-850, Istanbul, Turkey, 1998.
[3] Savov, V., N., Georgiev, Zh., D., Bogdanov, E., S., Analysis of the Magnetic Field in a Permanent Magnet Motor Carried Out by the Finite Element Method. Archive für Elektrotechnik, Vol.72, pp. 1-5, 1989.
[4] Üstün, Ö., Tunçay, R., N., Determination of Optimum Design Criteria of Coreless-Linear Brushless D.C. Machine, ISEF'99, Pavia, Italy, 1999.
[5] Chalmers, B., J., Tunçay R., N., Penman, J., Kamar, A., Studies of a Linear Induction Motor with Unlaminated Secondary, ICEM'78, Vol 2/2, Brussels, Belgium.
[6] Laithwaite, E., R., Linear Electric Machines- A Personal View, Proc. I.E.E.E., Vol.63, No 2, February 1976.
[7] Üstün, Ö., Robot Sürüşü İçin Doğrusal Asenkron Motor Tasarımı, Yüksek lisans tezi, I.T.Ü., Turkey, 1993.